MINIMIZATION OF COGGING TORQUE IN AXIAL FLUX PERMANENT MAGNET BRUSHLESS MOTOR WITH CERTAIN DESIGN

J. JENCY JOSEPH
Research Scholar, Anna University, Chennai, India
jency.joseph@yahoo.com

T. ARULDOSS ALBERT VICTOIRE
Associate Professor, Anna University Regional Centre, Coimbatore, Tamil Nadu, India
t.aruldoss@gmail.com

Abstract: *This paper deals with performance of an Axial Flux Permanent Magnet Brushless Motor for the low speed applications. Axial Flux Permanent Magnet Machines are high torque density motors and suitable for Electric Vehicles which reduces the total energy consumption for personal transportation. Normally the rated power of electric motor for Electric Vehicle varies from 10 to 75kW. For the investigation, 26kW single sided Axial Flux Machine has been taken and designed using Finite Element Method. The cogging torque is also minimized for the single stator-single rotor Axial Flux Permanent Magnet Motor which will improve the torque density of the motor to meet the requirements of Electric Vehicles at low speed conditions.*

Key words: *Axial Flux Permanent Magnet Brushless Motor (AFPMBLM) - Electric Vehicles (EV)-Single stator and single rotor (SSSR)-Cogging Torque Minimization(CTM)*

1. Introduction

In recent years, the electric vehicles are very popular for low speed applications. In all Major cities the enormous number of vehicles are running which reduces the transportation efficiency by taking too much of time to travel from one point to another and also increases the emission of toxic gases and smoke which leads to global warming. The correct alternative for the above problem is the use of Electric Vehicles which does not emit any toxic gases or smoke, as it uses clean energy source. Electric vehicles are of three major categories: Hybrid Electric Vehicles, Battery Electric Vehicles and Fuel Cell Eclectic Vehicles. Electric Motor assists the gasoline engine in Hybrid Electric Vehicles, in low speeds. The requirements of electric motor for HEVs are compact size and high torque density. In Battery Electric Vehicles the storage batteries are used as a source. The requirements of BEVs are compact size of hub motor. The requirements of all Electric Vehicles are perfectly satisfied by Axial Flux Permanent Magnet Brushless Motor which has high torque density. When compared to the radial-flux motor, axial-flux motor [1] has some features such as balanced motor-stator attractive forces, better heat removal configuration, no rotor back iron and adjustable air gap, etc. Axial-flux machines are different from conventional electrical machines in terms of the direction of the flux. The current is given to the stator coil. It may be DC current or AC current. If it is a DC Current, machine will act as a DC motor. If it is a AC current, the machine will act as the synchronous motor i.e. AC motor. The current flowing through each stator coil interacts with the flux created by the magnets on the rotor, producing a force tangential to the rotor circumference. The torque of electric motors is produced by the rate of change of the magnetic energy stored in the air gap. Based on the construction there are so many topologies in AF Motors. There are single sided, double sided and multisided machine topologies. Multisided topology has NN (North and the North pole facing) and NS (North and South pole facing) configurations.[2] Among all the topologies single sided AFPM Machine with slotted stator is considered for the investigation. It is necessary to make two assumptions:[3], (1) the motor is operated in the linear range of the B-H curve of magnetic material, (2) the flux flows straight across the air-gaps between the stator and rotor, ignoring the fringing flux for simplified analysis.

2. Design Variables

As discussed by several researchers [1-10], stator inner and outer diameters are the two most important design parameters. The ratio of inner and outer diameter, K_d is the key parameter to consider and it has a crucial impact on the determination of the machine characteristics, such as torque, torque to

weight ratio, iron losses, copper losses, and efficiency. Other important design parameters are the pole number, magnet thickness, conductor size, number of turns and material types. Nevertheless, the most restricting limitation for the number of poles is the motor operating speed. If the speed is high, a large number of poles will bring about an increase in the frequency [4, 6-10, 13], which directly leads to higher stator core losses and higher converter losses. The volume, thickness, shape and type of the permanent magnets also affect both the performance and the cost of the machine. The increasing number of stator poles N_s and larger outer radius R_o produce larger torques and higher efficiencies. On the contrary, a smaller inner radius R_i of stator poles allows larger magnetic flux distribution in the air gap to produce torque and hence efficiency.

3.Single Stator And Single Rotor Axial Flux Motor

Like the conventional DC motor, AFMs consists of both stator and rotor. Instead of field winding, the rotor consists of permanent magnet to produce the magnetic field which reduces the field copper loss. The magnets are surface mounted to produce a magnetic field which is directed in the axial direction in the machine air gaps. The easiest and the cheapest construction is the single-sided Machine (one rotor and one stator disk type). But, the high attractive force between the rotor and the stator can be counter balanced by the use of a second stator/rotor mounted as the mirror image of the first. This is called the double-sided arrangement. Double-sided model can be with an internal stator or an internal PM disk rotor. The toroidal core can either have radially directed slots or slot less. The slots being placed on either side of the core facing an air gap-in order to accommodate the active portions of the coils. The output power is fixed to 26kW for SSSR topology and the dimensions are found using sizing equations [1]. The following equation is used to find out the motor dimensions [5],

$$D_{out} = \sqrt[3]{\frac{\in P_{out}}{\pi^2 k_D k_{\omega 1} n_s B_{mg} A_m \eta \cos\phi}} \quad (1)$$

In the above equation (1), D_{out} is the motor outer diameter,$\in$ is the phase EMF to phase voltage ratio, P_{out} is the motor output power, k_d isthe motor inner to outer diameter ratio, $k_{\omega 1}$ is the winding factor, n_s is the rated speed in radiance per second, B_{mg} is the specific magnetic loading, A_m is the Specific Electric loading, η is the efficiency of the motor, cos Φ is the power factor. The finite element analysis allows modeling of complicated geometries in two Dimensional and in three Dimensional, and gives accurate results without standing on many restricting assumptions. In this work standard Finite Element Package is used for the modeling of Axial Flux Motor .

4. Finite Element Package.

The finite element packages have mainly three components: Pre-processor, Solver and Post-processor. In **pre-processor** the finite element model is created. First, the geometric outlines have been drawn in Finite Element package. Then, material properties are assigned to the various regions of the model. Next, the current sources and the boundary conditions are applied to the model. Finally, the finite element mesh is created. In **solver part**, the finite element solution is conducted. Some of the packages have adaptive mesh options, where an error estimate is produced from the solution; the mesh is refined and the solution is repeated again. The procedure goes on iteratively until the required accuracy level is achieved. In the **post-processor**, magnetic field quantities are displayed, and it allows calculating quantities, such as, force, energy and flux. The finite element analyses on the preliminary design prototype become necessary to provide detailed information on the magnetic flux and torque distribution, steady-state temperature distribution and modal dynamics. The dimensions are given in the table 1.

4. Two Dimensional and Three Dimensional Modeling

The Three dimensional motor structures can be simplified to a two dimensional configuration, and its fan shaped magnets are mapped into rectangular ones the arc is transformed to a straight line in the two dimensional linear motor model. Therefore, the total flux through the same area of magnet surface is unchanged. According to the dimensions given in table 1, model is drawn and it is shown in Figure 1. It shows the one portion of the full model, which contains the three stator teeth and two magnets.

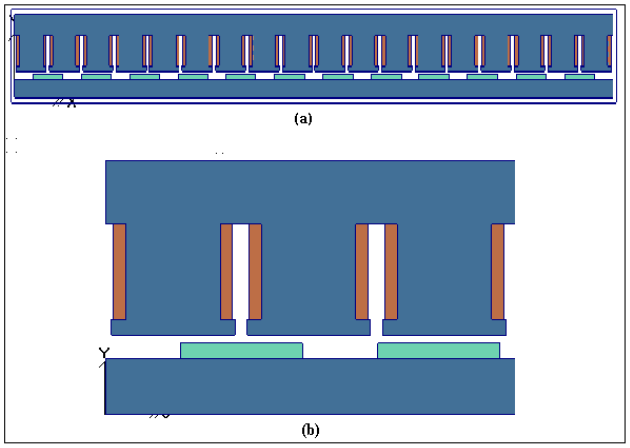

Fig. 1. a. Two dimensional model of AFPM, b. expanded view

The value of the flux density in various machine parts is an important variable in the design. It is the determining parameter in both core losses and the amount of saturation to which the machine is exposed. The exposure of the varying flux density at various machine parts is studied with the use of FEM. The flux density distributions are shown in Figure2.

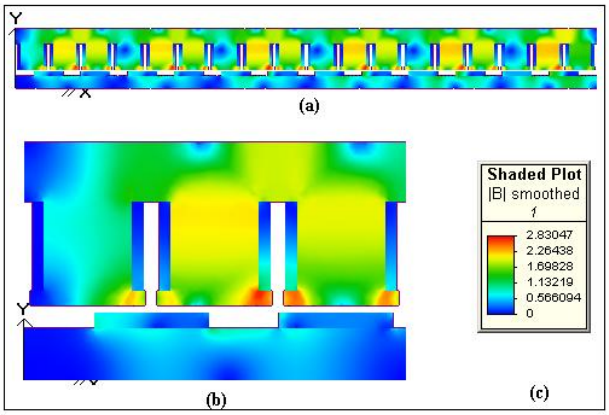

Fig. 2. a. Field diagram, b. expanded view, c.flux density values

It is clearly seen that the flux density values at different cross-sections of the machines are not equal. These differences are taken into account in the core loss calculations as well as in the prediction of the machine performance. The flux pattern for the AFPM is shown in figure 3. From this the direction of the flux can be easily identified. Flux is starting from the magnet according to the orientation and passing through the air gap and reaches the stator, so that the closed loop is formed.

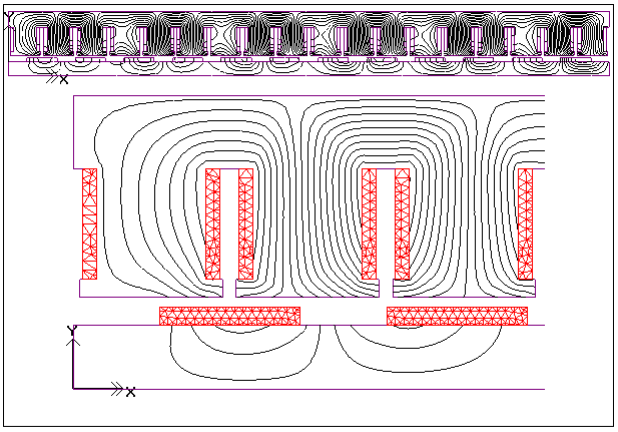

Fig. 3. Flux pattern with Expanded View

Three dimensional modeling is the accurate procedure to model the AFPM machines because of the direction of the flux, which flows in the Z-axis. For this purpose 3D static solver is used to find the back EMF and torque waveform. The three dimensional model of AFPM is shown in Figure 4.

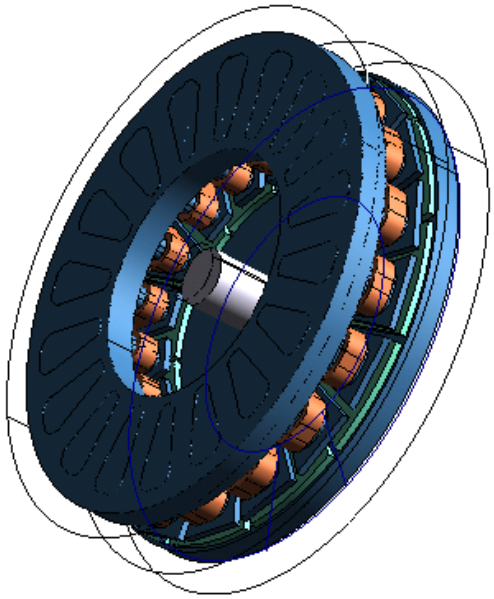

Fig. 4. Three Dimentional Model of single side stator and rotor

Initially the stator is not excited. Due to the flux produced by the magnets, there is a flux linkage in the stator coils. From the flux linkage, the back emf is calculated and it is given in Figure 5.

The flux density of each part is shown in the Figure 6. The flux density in each part is differing from other part. This is the main factor to produce the

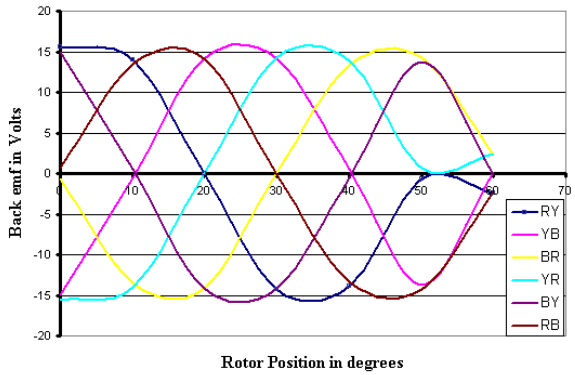

Fig. 5. Back EMF waveform with rotor Position

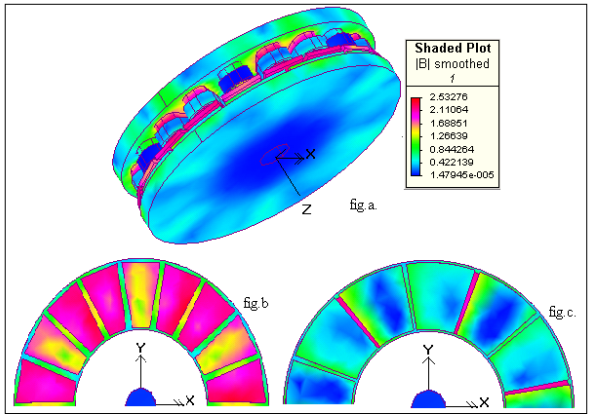

Fig. 6. a) Flux density for full model with values, b) stator, c) rotor magnets

the torque. The core losses are also depends on this flux density. It should be minimum at the shoes to avoid excess of core losses. The shoes should be protected from saturation. Due to the interaction between the stator and rotor magnetic field there is a force exerted on the rotor surface. The cumulative force produces the torque, which is used to overcome the losses. The torque plot is given in the Figure 7.The maximum torque for the designed single sided rotor and stator model is 22.3Nm at the rotation angle of 20degree. For each 60 degree this plot is repeated because 60 degree mechanical is equivalent to 360 degree electrical. The design parameters are varied to get the maximum torque. The air gaps, length of the magnet, stator current number of turns are varied to get the optimum design [3]. These are checked for maximum torque with minimum saturation. The designed model produces the maximum flux density at the shoes of 2.11T with the air gap flux density of 0.59T, and the Maximum torque is 22.3Nm. By changing the no of turns, stator current, length of the air gap, Magnet length and arc suspended by the rotor, the different configurations can be achieved. The torque values for different configurations of AFPM machine are shown in Table.2. When changing the design parameter the torque values are also changed. When angle suspended by the magnet is increased, the torque will be very high which is about 33.7Nm which is shown in Table 2. The double-sided type of AFPM is shown in Figure 8. With double sided AFPM design, the torque value is doubled which is of about 66.46Nm. When the trapezoidal magnet is used the torque is increased to 34.8Nm. But there are some design difficulties in the trapezoidal type. But there is some design difficulties in the trapezoidal type. The comparison torque graph for different configuration is given in the Figure 9.

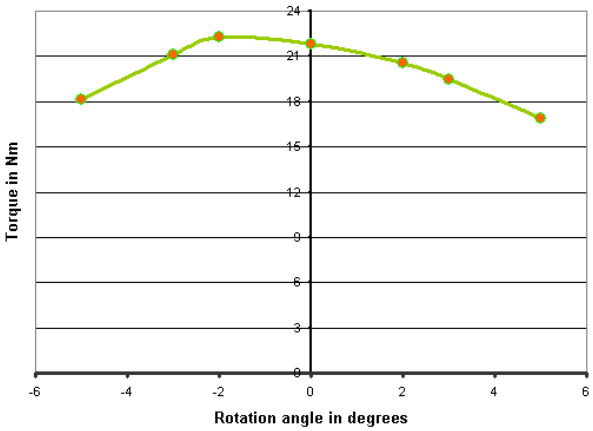

Fig. 7. Torque Plot for Single side rotor and stator with rotor position

The configurations are numbered in table 3. The configurations are as follows,

1. The angle suspended by the magnet is 13 degrees
2. The angle suspended by the magnet is 14 degrees
3. The angle suspended by the magnet is 13 degrees and double sided.
4. The angle suspended by the magnet is 14 degrees and outer radius is 69mm
5. The angle suspended by the magnet is 9 degrees; Back iron thickness is 3.5 mm
6. The angle suspended by the magnet is 9 degrees; Back iron thickness is 7 mm
7. The angle suspended by the trapezoidal magnet is 14 degrees.

5. Analytical validation

The results from the simulation are validated by analytical calculation. These calculations are handled using the magnetic circuit analysis. Here, one assumption is made; there is no leakage flux and no fringing effect. Finally the simulation results and

analytical results are compared. The magnetic circuit is

Table 1
Machine Specifications

Sl.No	Geometric dimensions	Values
1	Number of stator poles	18
2	Number of magnets	12
3	Air gap length(mm)	1
4	Rotor thickness(mm)	7.5
5	Shoe depth(mm)	2
6	Shoe width(mm)	20
7	Tooth height(mm)	24
8	No. of coils per tooth	148
9	Outer radius(mm)	66
10	Inner radius(mm)	34
11	Back iron width(mm)	8

drawn for one electrical 360 degree, which is equivalent to 60 mechanical degrees.

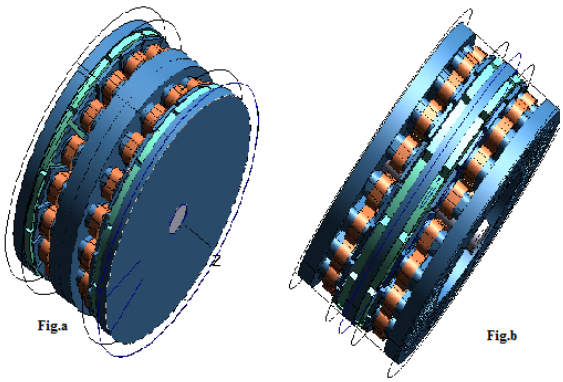

Fig. 8. Double sided model a)Internal Stator, Internal Rotor Machine

This portion consists of three stator teeth and two magnets. Figure 10 shows the magnetic circuit for AFPM which is only for mechanical 60 degrees. This circuit is repeated every 60 degrees. In this Figure R represents the reluctance of each portion. And the source is mmf source. The reluctance of each portions are calculated using the dimensions separately**.** Mesh equation method is used to find the loop flux. Using the torque equations, the electromagnetic torque (T_{em}) can be calculated

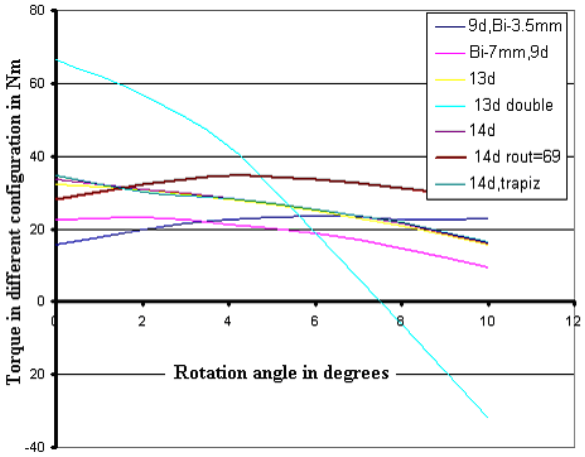

Fig. 9. Torque plot for different configuration with respect to rotation angle

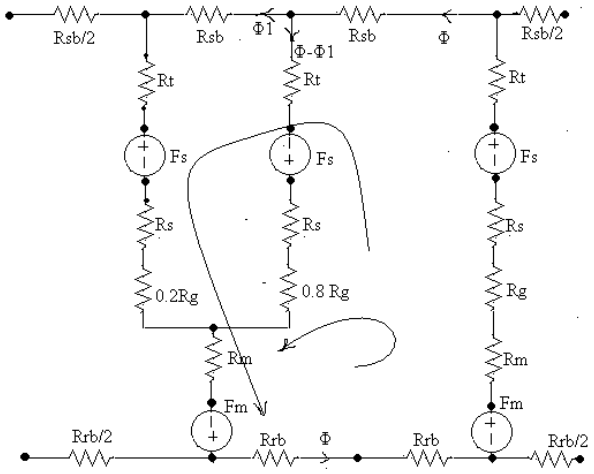

Fig. 10 . Magnetic Circuit For one mechanical 60 degrees

Table.2.
Comparison of Torque values for Different configurations

No. of Turns	Stator current	Air gap	Magnet length	Arc suspended By the magnet	Maximum Flux density	Air-gap flux density	Torque
148T	20A	1mm	4mm	9deg	1.09T	0.489T	23.46Nm
148T	20A	1.5mm	2mm	28deg	2.11T	0.59T	22.3Nm
100T	10A	1mm	4mm	28deg	2.00T	0.699T	26.87Nm
100T	10A	1.5mm	2mm	28deg	0.96T	0.767T	14.8Nm

Table .3.

Torque Values for Different configurations with respect to the angle suspended by the rotor Magnets

Rotation Angle in degrees	Different Configurations 1	2	3	4	5	6	7
0	32.2	33.7	66.4	28.1	15.5	22.6	34.8
2	30.9	30.7	56.7	32.2	19.7	23.3	30.3
4	28.3	28.4	42.6	34.6	22.5	21.3	28.5
6	25.1	25.4	18.7	33.7	23.5	18.7	25.2
8	20.8	21.4	-6.1	31.3	22.5	14.7	21.7
10	15.6	16.1	-32.1	28.4	22.9	9.5	16.3

The linear current density on the inner radius of the machine is calculated using the formula

$$A_{in} = \frac{m \times N_{ph} \times I}{\pi \times r_{in}} \quad (2)$$

$$T_{em} = \pi \times B_{\max} \times A_{in} \times \left[1 - k_D^2\right] \times r_{out}^{\,3} \times k_D \quad (3)$$

$k_D = 0.53$, substitute all the values in the above equations, T_{em} value is 23.4 Nm. A torque value, which is calculated by the analytical calculation[1], is compared with the simulation results and the percentage error is calculated. The values are predicted in table 4.

6. Minimization of Cogging Torque

Torque quality is a very important issue for the electric drives. There are two undesired pulsating torque components in PMs which affect the machine performance. One of which is ripple torque, it is due to harmonic content of the machine voltage and current waveforms. Other is cogging torque caused by the attraction between the rotor magnetic field and angular variations of the stator reluctance. [11]

Table 4
Results of magnetic circuit analysis

Terms	Simulation Results	Analytical results
Air gap flux	0.59034Wb	0.84Wb
Flux linkage	0.037356WbT	0.0926 Wb T
Electromagnetic torque(T_{em})	22.3Nm	23.4Nm
Percentage error in electromagnetic torque	**4.7%**	

These components not only affect the self-starting ability of the motor but also produce the noise and mechanical vibrations. Cogging torque is estimated

by calculating the change of total energy stored in the air gap with respect to the rotor position and can be written as[11]

$$T_{ag}(\theta r) = \frac{1}{2} \times \phi_g^{\,2} \times \frac{dR}{d\theta} \qquad (4)$$

ϕ_g is the flux is the air gap, R is the air gap reluctance and θ_r is the angular rotor position. However, the cogging torque fundamentally results from the non-uniform flux distribution in the air gap. As the teeth become saturated, the flux begins to distribute more evenly in the air gap and the cogging torque decreases**.** Many techniques are used to minimize the cogging torque which is illustrated in many literatures for PM machines. These techniques include magnet pole shape, skewing stator tooth or rotor magnets, magnet or pole shifting, pole-arc ratio and stator slot design, etc. Most of the techniques mentioned can be applied to AFM. As per the survey, the cogging torque minimization technique especially for axial flux PM machine structure called alternating magnet pole-arc[11] method is proposed for single stator single rotor model. In this method, consequent magnet in rotor is designed with two different magnet pole-arc ratios as shown in figure 11. The consequent magnets in rotor are designed with two different magnet pole-arc ratios: α_m and α_c. The objective of this technique is to vary the cogging torque phase angle by alternatively using two magnet pole arcs and simultaneously to reduce the amplitude of each portion so that the superposition of the cogging torque variation of all air gap adds up to a very small value.

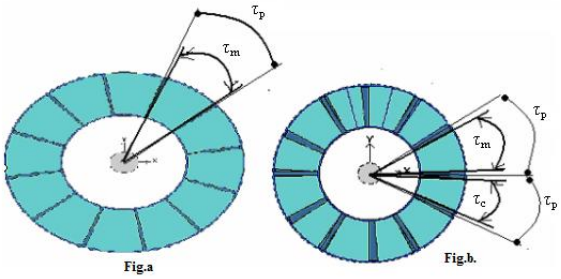

Fig. 11. Alternating Magnet pole arcs, (a) same pole arcs, (b) alternating pole arc

It should also be mentioned that the definition of magnet pole-arc is given by the ratio of magnet pitch to rotor pole pitch, i.e.

$$\alpha_m = \frac{\tau_m}{\tau_p} \quad \text{and} \quad \alpha_c = \frac{\tau_c}{\tau_p} \qquad (5)$$

Where τ_m and τ_c are the magnet pitches and τ_p is the rotor pole pitch.

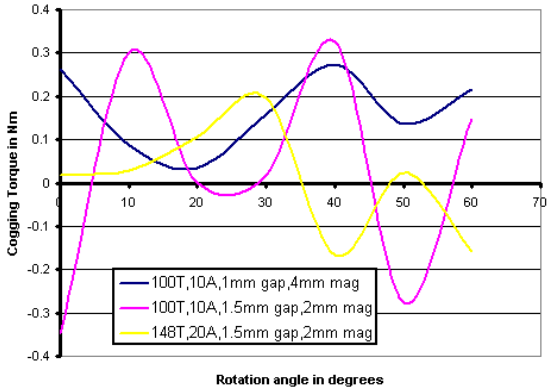

Fig.12. Cogging Torque for three different configurations of AFPM machines

Before applying the technique, the suitable design have to be selected. When the machine is designed with 148T,20A,1.5mm air gap and 2mm magnet the flux density at the shoe is high and due to this saturation, there is an even flux distribution and the cogging torque decreases which is shown in yellow color waveform in the figure 12. When the machine is designed with 100T,10A, 1.5mm air gap and 2mm magnet ,the flux density is somewhat reduced. Due to this there is an un-even flux distribution and the cogging torque is increased. So this design is taken and the minimization technique is applied to this design. The maximum magnet pitch for τ_m and τ_c is 30° (mechanical). Both magnet pitches are considered as variables not only to attain the minimum cogging torque for the designed dimensions and pole numbers but to prove the feasibility of the proposed technique as well. The different values used in finite element analysis and the values which are taken as the positive peak value in each graph is listed in the Table.5.

From this table the minimum values are selected and the graph for those values is given in the Figure 13. The table shows that different combinations of τ_m / τ_c ratio offer reasonable small cogging torque compared to the case where both pole-arcs are the same**.** The Yellow line in Figure 13 gives the minimum cogging torque. The pole arc ratio corresponding that graph is 0.5. ($\tau_m = 20$, and $\tau_c = 10$ (mechanical degree)). The cogging torque before the technique applied and after the technique used is given in the Table 6.

Table 5
Different Magnet Pole pitch values used for Analysis

τ_c \ τ_m	5	10	15	20	25	30
5	-0.0301	-0.0333	0.1122	**0.0356**	0.0678	**0.0359**
10		0.0703	0.2602	**0.0205**	0.1176	0.0732
15			0.0715	0.0446	0.1739	0.1076
20				0.3571	0.0764	0.0517
25					-0.2212	0.1056
30						0.0811

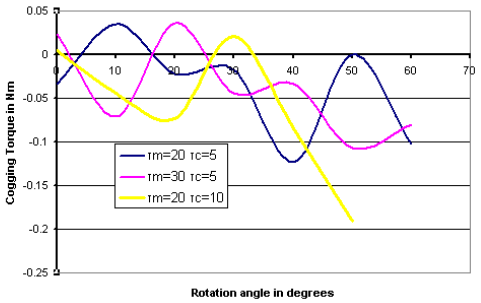

Fig. 13. Coggoing Torque for different values of magnet pole pitches after applying alternating pole arc method

Table.6.
Percentage reduction in cogging torque

Cogging torque before the Technique is used	Cogging torque after the technique is used	Percentage reduction in cogging torque
0.32	**0.021**	**93.43%**

From the above table, it is shown that the cogging torque is reduced to 93.43% of the original value. Similarly the overall torque also increased corresponding to the reduction in the cogging torque.

7. Conclusion

Performance of Axial Flux Permanent Magnet Machine has been studied with different configurations. In this work the design parameters have been changed randomly and the results were taken and compared. It will be very useful for the basic analysis of Axial Flux Permanent Magnet Motor. So many models were created, For the 148T turns, 20A stator current, 1.5mm air-gap, 2mm magnet thickness, 28 degree magnet arc model the air gap flux, flux linkage and electromagnetic torque are validated using Magnetic Circuit Analysis. It is proved that the double sided machine topology gives double the amount of torque which is very useful for high power range of electric vehicles. Torque density is the very important requirement for the wheel motors. To maintain the quality of the torque density the cogging torque should be reduced. In this work, using FEM, Alternating magnet pole-arc Method[11] is applied to minimize the cogging torque. After applying this method for single rotor single stator the cogging torque is reduced by the amount 93.43% which will increase the overall torque quality of the motor. By improving the torque density these motors can be the suitable alternative for the conventional electric motor for electric vehicle applications in low speed range.

References

1. Asko Parviainen:*Design Of Axial-Flux Permanent Magnet Low-Speed Machines And Performance Comparison Between Radial-Flux And Axial-Flux Machines*. Ph.D. Thesis, Lappeenranta University of Technology, Finland, April, 2005.
2. Ju Hyung Kim,Wooyoung Choi, Bulent Sarlioglu: *Closed-Form Solution for Axial Flux Permanent-Magnet Machines With a Traction Application Study*, IEEE Transactions on Industry Applications,vol.52,No. 2, March/April 2016.
3. Y.P.Yang, C.H.Cheung, S.W.Wu, J.P.Wang:*Optimal Design And Control Of Axial-Flux Brushless DC Wheel Motor For Electrical Vehicles*,Proceedings of the 10th Mediterranean Conference, Lisbon, Portugal, July, 2002
4. Ahmad Darabi, Hassan Moradi and Hossein Azarinfar:*Design and Simulation of Low Speed Axial Flux Permanent Magnet Machine*,World Academy of Science, Engineering and Technology 61,2012, pp. 692-695.
5. Jacek F.Gieras,Rong-Jie Wang, Maarten J.Kamper:*Axial Flux Permanent Magnet Brushless Machines",* 2 nd Edition ,Springer, 2008.
6. Metin Aydin,Surong Huang and Thomas A. Lipo: *Design,Analysis and Control of a Hybrid Field-Controlled Axial-Flux Permanent-Magnet Motor*, IEEE Transactions on Industrial Electronics,vol 57,no.1, January 2010,pp.78-87.
7. Tae-Suk Kwon, Seung-Ki Sul, Luigi Alberti and Nicola Bianchi:*Design and Control of an Axial-Flux Machine for a Wide Flux-Weakening Operation Region*", IEEE Transactions on Industry applications,vol.45,no4,July/August 2009, pp. 1258-1266.
8. Rong-Jie Wang, Maarten J. Kamper, Kobus Van and Jacek F.Gieras: *Optimal Design of a Coreless Stator Axial Flux Permanent-Magnet Generator*, IEEE Transactions on Magnetics, vol.41, no.1, January 2005,pp.55-64.
9. Andrew S.Holmes, Guodong Hong and Keith R. Pullen: *Axial-Flux Permanent Magnet Machines for Micro power Generation*,Journal of Microelectromechanical Systems, vol.14,no.1,February 2005, pp. 54-62
10. Asko Parviainen, Markku Niemela and Juha Pyrhonen: *Modeling Of Axial-Flux Permanent-Magnet Machines*,IEEE Transactions on Industry Applications, Vol.40, No.5, September/October 2004, pp.1333-1340
11. Metin Aydin, Ronghai Qu and Thomas A. Lipo: *Cogging Torque Minimization Technique For Multiple-Rotor, Axial-Flux Surface-Mounted-PM Motors, Alternating Magnet Pole-Arcs In Facing Rotors*. University of Wisconsin, Madison, 2003 IEEE, pp.555-561.
12. Jenni pippuri,Aino manninen, Janne Keranen,and Kari Tammi:*Torque Density of Radial, Axial and Transverse Flux Permanent Magnet Machine Topologies*, IEEE Transactions On Magnetics, vol. 49, no. 5, May 2013 pp. 2339-2342
13. Federico Cariccchi, Fabio Recombine, Ezio Santini,*Basic Principle And Design Criteria Of AFPM Machines Having Counter Rotating Rotors*.IEEE Transaction on Industry Applications, Vol.31, N0.5, September/October 1995, pp.1062-1068